# Identification of Non-Restorative Sleep Associated with Depression Using Ambulatory Electrocardiogram and Triaxial Acceleration

Li Liu, Chongyang Wang, Guangyuan Liu, Wanhui Wen*

***Abstract*— Objective: Non-restorative sleep is prevalent among individuals with depression and is strongly associated with the severity of the condition. Therefore, identifying non-restorative sleep can aid in the early screening of depression. Investigating non-restorative sleep in depression necessitates long-term monitoring under naturalistic conditions. Methods: In this study, we recruited 149 participants and collected electrocardiogram and triaxial acceleration from them, resulting in a total of 761 nights of data. The period from midnight to 6:30 AM was segmented into 78 five-minute intervals, from which 40 physiological features were extracted for each interval. To deal with variations in sleep patterns across participants and dates, we reordered the sleep data based on levels of parasympathetic nervous system (PNS) activation to explore the underlying neural mechanisms of non-restorative sleep in individuals with depressive symptoms. Results: We developed a model that integrated convolutional neural networks with an attention mechanism to identify non-restorative sleep in individuals with depressive symptoms. The model demonstrated impressive performance on an independent test set, achieving an accuracy of 81.25% and an F1 score of 77.85%. Additionally, Bayes' theorem was used to compute the posterior probability indicating non-restorative sleep in this population, assessing abnormal PNS activation. Conclusion: Finally, we designed a system capable of automatically evaluating nighttime sleep status and quantifying changes in non-restorative sleep associated with depression. Significance: This system offers a novel tool and method for the early identification of individuals at risk of depression.**

***Index Terms*— Parasympathetic Nervous System; Depression; Non-Restorative Sleep; Machine Learning; Depressive Symptom Evaluation**

## I. Introduction

DEPRESSION is a prevalent disorder frequently co-occurring with various mental and physical conditions, ranking among the top ten global diseases. The estimated prevalence of major depressive disorder in the general population ranges from 4.4% to 20% [1]. Despite advancements in treatment, many depressed individuals, particularly younger populations, continue to experience inadequate relief from existing psychological and pharmacological interventions [2], [3]. Furthermore, progress in early intervention for depression remains insufficient due to the inconvenient early screening of depression in the general population [2], [3]. Commonly used depression screening tools, such as the Beck Depression Inventory, Patient Health Questionnaire-9, and Self-Rating Depression Scale (SDS), rely on active self-reporting. These tools are not ideal for frequent, short-term assessments, thus highlighting a need for more convenient daily-use instruments.

Studies have shown that different subtypes of depression exhibit varying degrees of circadian rhythm disturbances, manifesting as abnormal sleep-wake cycles, extended sleep duration, non-restorative sleep (NRS), excessive daytime inactivity, and irregular sleep onset and offset time [4]–[7]. Sleep disturbances are prominent in patients with circadian rhythm-related depressive symptoms [8]–[10], with approximately 90% of depressed patients experiencing sleep issues such as insomnia, NRS, hypersomnia, and narcolepsy [11], [12]. Among these, NRS is notably prevalent [13]. NRS is typically characterized by a subjective sense of unrefreshing sleep upon awakening, often resulting from poor sleep quality or restlessness [14]. This type of impaired sleep can exacerbate daytime anxiety or depressive symptoms [15], [16], significantly affecting overall mental health [17], and may even lead to suicidal ideation [18].

Improving sleep quality has been linked to remission and recovery from depression, with evidence suggesting that addressing insomnia can prevent both the onset and recurrence of depressive episodes [19]. The connection between NRS and circadian rhythm disruptions provides a crucial entry point for early screening of specific depressive symptoms [20]. Identifying individuals with depressive NRS can facilitate early detection and intervention. Monitoring the neurophysiological mechanisms underlying depressive NRS enables targeted regulation of the biological clock, potentially reducing the occurrence of NRS and, consequently, the severity and recurrence of depressive symptoms.

There is a growing interest in using resting-state EEG signals to explore sleep status in depressed individuals [21]–[23]. Although comparing sleep stages of depressed and non-

• Wanhui Wen is the corresponding author.
• Li Liu, Guangyuan Liu, Wanhui Wen are with the Chongqing Key Laboratory of Generic Technology and System of Service Robots, Chongqing Key Laboratory of Nonlinear Circuits and Intelligent Information Processing, and the College of Electronic and Information Engineering, Southwest University, Chongqing, 400715, China (e-mail: 2534997991@qq.com, liugy@swu.edu.cn, cwenwanh@swu.edu.cn). Chongyang Wang is with the Key Laboratory of Rehabilitation Medicine in Sichuan Province, Department of Rehabilitation Medicine, and Institute of Rehabilitation Medicine, West China Hospital, Sichuan University, Chengdu, 610041, China (e-mail: mvrjustid@gmail.com).

depressed individuals can yield valuable insights, the practical application of EEG is limited by the stringent experimental controls required and the high cost of EEG equipment, which is not feasible for general household use. In contrast, ECG data collection is more accessible and cost-effective. The R wave to R wave (RR) interval in ECG signals, reflecting heart rate rhythm controlled by both sympathetic and parasympathetic branches of the autonomic nervous system [22]–[26], presents a reliable method for exploring sleep characteristics in individuals with depression [24], [25].

Existing research often focuses on diagnosed patients with depressive disorder and fails to address early screening before symptom exacerbation, particularly overlooking NRS associated with circadian rhythm disruptions [27]. Moreover, data collected in controlled laboratory or hospital settings may not accurately reflect real-world conditions [26]. The variability in sleep conditions across individuals and dates poses challenges for comparability.

Given the critical role of deep sleep in brain metabolism recovery and neural stability [28], [29], as well as the predominance of parasympathetic activity during this sleep phase [30], this work proposes aligning sleep conditions across different individuals and nights based on parasympathetic nervous system (PNS) activation levels, as reflected by high-frequency features in heart rate variability (HRV). We further introduce a model designed to identify NRS in individuals with depression by analyzing nocturnal physiological data. This model provides a tool for recognizing individuals with circadian rhythm-related depressive symptoms. Additionally, Bayes' theorem was applied to compute the posterior probability of NRS status, thus quantifying the impact of circadian rhythm-related depression. Finally, we developed a system capable of automatically identifying and quantifying NRS in individuals exhibiting circadian rhythm-related depressive symptoms.

## II. MATERIALS AND METHODS

This section provides a detailed account of the data collection process, preprocessing steps, and the specific techniques employed for feature extraction and statistical analysis. We outline the comprehensive approach used to assess non-restorative sleep associated with depression (NRSD). Additionally, we describe the machine learning methodologies utilized to identify NRSD and explain the application of Bayes' theorem to compute posterior probabilities, thereby quantifying the extent of abnormal nocturnal PNS activity within the NRSD population.

### A. Assessment of NRSD

We utilized the SDS [31] to assess depressive symptoms of the participants. SDS comprises 20 items, each rated on a four-point scale reflecting the frequency of symptoms. According to Chinese norms [32], [33], a standard SDS score of 53 points serves as the cutoff for depression: scores ranging from 53 to 62 indicate mild depression, 63 to 72 indicate moderate depression, and scores above 73 indicate severe depression.

Participants' sleep quality on the night of data collection was rated on a scale from 1 to 5, with 1 indicating poor sleep quality and 5 indicating excellent sleep quality. Higher scores correspond to better sleep quality. Scores of 1-2 are considered indicative of NRS, while scores of 4-5 are classified as restorative sleep. Due to the subjective nature of this rating, a score of 3 is interpreted as reflecting uncertain sleep quality.

Each participant completed the SDS scale twice: once at the beginning of physiological data collection and once at the end. Additionally, participants kept a daily activity log, recording their sleep and wake time. Participants whose SDS scores exceeded 53 in both assessments and who reported poor sleep quality (scoring 1–2 points) on at least four nights per week were categorized as 'with NRSD'. The control group consisted of three subgroups: 1. Participants whose SDS scores were consistently below 53 in both assessments and who reported normal sleep quality (scoring 4–5 points) on at least four nights per week (normal subgroup). 2. Participants whose SDS scores were higher than 53 in both assessments but who reported normal sleep quality (scoring 4–5 points) on at least four nights per week (subgroup with depression but no NRS). 3. Participants whose SDS scores were below 53 in both assessments but who reported poor sleep quality (scoring 1–2 points) on at least four nights per week (subgroup with NRS but no depression).

### B. Data Collection

We recruited 149 undergraduate and graduate students from Southwest University for data collection. Participants had no history of heart disease or mental illness and did not use nerve stimulants, depressants, or sleep-related medications during the study. All participants provided informed consent prior to the experiment. Among these participants, 48 took part in two data collection sessions spaced three to six months apart, with 27 showing changes in their condition between sessions.

Prior to physiological data collection, participants completed the SDS scale to assess their depressive symptoms. Following this initial assessment, we collected ambulatory ECG and tri-axial accelerometer (T-ACC) data over several days, along with participants' daily self-reports of sleep quality. On the final day of the experiment, participants completed the SDS scale again for a follow-up assessment of depressive symptoms.

Data collection was conducted using Shimmer3 devices, which recorded ECG and T-ACC data synchronously at a sampling frequency of 512 Hz. The Shimmer3 device was attached to participants' waists with an elastic band, and five silver chloride electrode patches were placed on their chests following the Shimmer3 user manual. The Vx lead was selected for subsequent data analysis due to its higher R-wave amplitude, facilitating accurate R-wave peak detection.

Throughout the data collection period, participants were free to engage in their usual daily activities without restrictions, allowing them to work and rest according to their own schedules and preferences. To mitigate data quality issues related to electrode failure, participants were advised to avoid excessive sweating from vigorous exercise. Finally, we successfully collected ECG and T-ACC data from 149 participants over a total

TABLE I: Details of data collection

| Label | $N_s$ | $N_d$ | $N_{s\_f}$ | $N_{d\_f}$ | $N_{s\_m}$ | $N_{d\_m}$ |
|---|---|---|---|---|---|---|
| With NRSD$^E$ | 72 | 318 | 40 | 180 | 32 | 138 |
| Normal$^{C1}$ | 73 | 316 | 45 | 202 | 28 | 114 |
| With depression but no NRS$^{C2}$ | 22 | 91 | 9 | 36 | 13 | 55 |
| With NRS but no depression$^{C3}$ | 9 | 36 | 3 | 11 | 6 | 25 |

E: experiment group; C1, C2 and C3: three control subgroups; $N_s$: total number of subjects; $N_d$: total number of days of data collection; $N_{s\_f}$: number of male subjects; $N_{d\_f}$: number of days of data collection for male subjects; $N_{s\_m}$: number of female subjects; $N_{d\_m}$: number of days of data collection for female subjects. Forty-eight participants took part in a follow-up session of data collection, and 27 of them were marked with different labels in two sessions of data collection.

of 761 days. Using the methodologies from the literature [34], we performed an initial quantification of the subjects' physiological circadian rhythms, followed by a post-measurement follow-up. Based on our quantitative assessments, participants evaluated their daytime states in relation to the restorative impact of nighttime sleep, specifically reporting on morning fatigue, low energy, and excessive daytime sleepiness. Following the post-test follow-up, and based on self-reported SDS and sleep quality scores, we categorized the data into an experimental group and three control subgroups, as shown in Table I.

### C. Physiological data preprocessing and Feature Extraction

We employed the wavelet decomposition and reconstruction method, as proposed in [35], to remove baseline drift from the ECG data and low-frequency trends from the T-ACC data. Subsequently, we applied an adaptive running window method [35] to automatically calculate RR intervals. Specifically, we set a dynamic running window length to be 1.3 to 1.5 times the previous normal RR interval. Within this window, the maximum value in the baseline-corrected ECG data was identified as the R-peak, and the time difference between consecutive R-peaks was computed to determine the RR interval. After obtaining the RR interval series in seconds, we converted it to a heart rate (HR) time series in beats per minute using the formula HR=60/NN, where NN represents the normal RR intervals, obtained by excluding occasional intervals caused by premature beats and their subsequent compensatory pauses from the RR interval series. These intervals were automatically removed during the fourth preprocessing step, as shown in Figure 1. Afterward, an experienced ECG technician reviewed the RR interval series and manually removed any remaining abnormal intervals, which were typically few in number.

Additionally, we processed the acceleration data by averaging the three-axis data (after removing low-frequency trends) to produce a composite signal, denoted AT-ACC, as illustrated in Figure 1.

We define the sleep start time as the point when a marked change in the amplitude pattern of AT-ACC data occurs, which is further verified given the self-reported start of sleep to avoid outlier mistakes. Similarly, the sleep end time is defined as the point when the AT-ACC amplitude pattern shifts significantly near the self-reported end of sleep. As illustrated in Figure 2, the AT-ACC data show substantially lower amplitude values and reduced spike density during sleep period compared to active periods. The sleep start and end timestamps are independently determined by an experienced AT-ACC data processing technician and subsequently reviewed and confirmed by another equally experienced technician. We calculated the participants' sleep onset and wake-up time, as illustrated in Figures 3 and 4. The majority of participants' sleep periods occurred between 00:00 and 06:30, aligning with typical physiological nocturnal rhythms as indicated by previous research [36]. Accordingly, our data analysis focused on this time frame, which we divided into 78 five-minute time slots. Within each slot, we extracted 36 HRV features and 4 AT-ACC features to assess participants' autonomic nervous activity and physical movement. This yielded a structured data matrix sized $40 \times 78$, where each row represented a physiological parameter and each column corresponded to a time slot. Specific details of the 40 physiological features are provided in Table II.

Given the variability in nighttime sleep duration across different populations and dates, aligning sleep stages for comparison presents a challenge. Several studies [37]–[39] underscore the role of the PNS in maintaining body homeostasis and improving insomnia and sleep quality. Moreover, the 'HF' feature listed in Table II has been demonstrated to reflect PNS activation [40]–[42]. Therefore, we sorted the 78 time slots from 00:00 to 06:30 based on the 'HF' feature values in descending order. This approach aims to reduce errors stemming from sleep stage misalignment during nocturnal periods, facilitating comparison between the NRSD group and the normal group based on PNS activation levels. Figure 5 illustrates the distribution of HF feature values within a single time slot for the NRSD group and the normal group. The distribution for the NRSD group is notably skewed towards the lower end, indicating reduced PNS activation compared to the normal group.

### D. Statistical Testing of Physiological Feature in Each Time Slot

The objective of the statistical analysis is to identify inter-group differences in physiological features between the NRSD group and the normal group. Given that the distribution of physiological feature values across most time slots did not conform to normality assumptions, we employed the non-parametric Mann-Whitney U test for analysis. Our null hypothesis posits that there are no significant differences in physiological feature values between the NRSD group and the normal group within specific time slots.

To visually represent the distribution of each physiological feature, we used box plots, with color coding to indicate statistical significance levels. Specifically, a pink color denotes a significance level of $0.001 < P \leq 0.05$, while a white color indicates $P > 0.05$. The P-value reflects the likelihood of the null hypothesis being true.

After identifying physiological features with significant inter-group differences through statistical testing, we employed

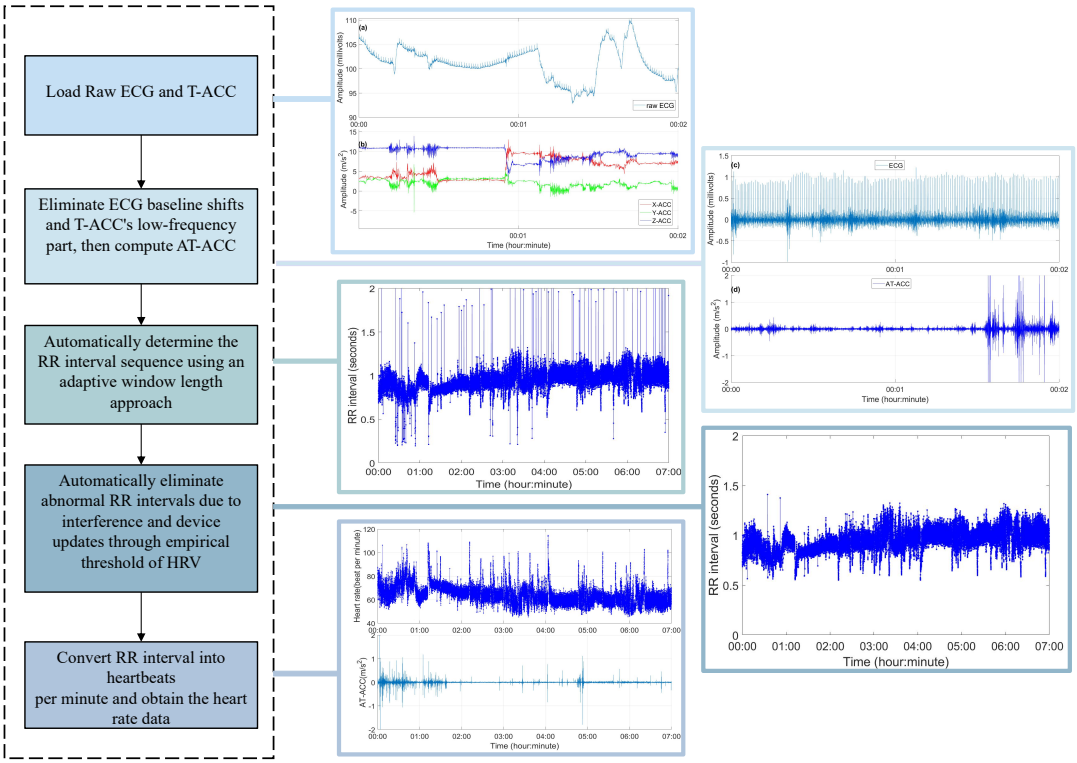


Fig. 1. Flowchart and illustrative results of ECG and T-ACC data preprocessing

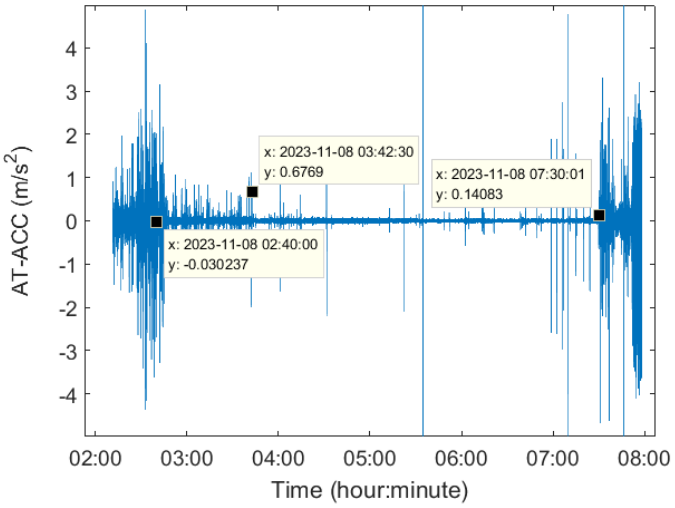


Fig. 2. AT-ACC data indicative of sleep onset and offset. The subject reported going to bed at 02:40 and waking up at 07:30. However, AT-ACC data indicated a sleep onset at 03:43 and a sleep offset at 07:30.

Bayesian theory to calculate the posterior probability of a specific observation sample belonging to the NRSD group, in order to assess the severity of NRSD symptoms in that sample. Specifically, for the 'HF' feature within a particular time slot, we used the Kernel Density Estimation (KDE) function [55] to fit the probability density distributions of the samples from the NRSD group and the normal group, as shown in Figure 5. These fitted distributions were then respectively used in formula (1) to compute the posterior probabilities of the current sample belonging to each group in that time slot.

$$\widehat{P}(G = j \mid \mathrm{HF} = x_0) = \frac{\widehat{\pi}_j \widehat{f}_j(x_0)}{\sum_{k=1}^{2} \widehat{\pi}_k \widehat{f}_k(x_0)} \tag{1}$$

Where $\hat{f}_k(x_0)$ is the KDE value of category $k(k = 1, 2)$ for a given value $x_0$ of the 'HF' feature, and the values 1 and 2 of $k$ corresponds to the categories 'with NRSD' and 'normal group'. $\widehat{\pi}_k(k = 1, 2)$ means the estimation of prior probability for category $k$, which is empirically set to be 0.5 for each of the categories. $\widehat{P}(G = j \mid \mathrm{HF} = x_0)$ is the estimation of posterior probability of the current sample's category $G$ being $j$ $(j = 1$ or $2)$ under the condition of $\mathrm{HF} = x_0$.

According to Formula (1), the sum of $\widehat{P}(G = 1|\mathrm{HF} = x_0)$ and $\widehat{P}(G = 2|\mathrm{HF} = x_0)$ equals 1. Therefore, if $\widehat{P}(G = 1|\mathrm{HF} = x_0)$ exceeds 0.5, it indicates that the sample is more likely to belong to the group with NRSD. Conversely, if $\widehat{P}(G = 1|\mathrm{HF} = x_0)$ is below 0.5, it suggests that the sample is more likely to belong to the normal group.

### *E. Deep Learning Approach for NRSD Recognition*

In this study, we employed a neural network model named CNN_ECAnet to classify data samples from individuals with and without NRSD. The core architecture of CNN_ECAnet comprises a Convolutional Neural Network (CNN) and an Efficient Channel Attention (ECA) layer, followed by a Fully Connected Neural Network (FCNN) with four fully connected layers.

Initially, the input data, a 40×78 matrix representing a full night's physiological feature values, is processed by the

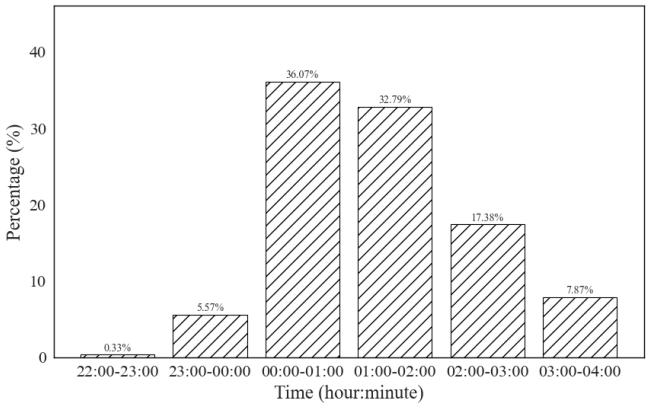


Fig. 3. Distribution of participants' sleep onset time

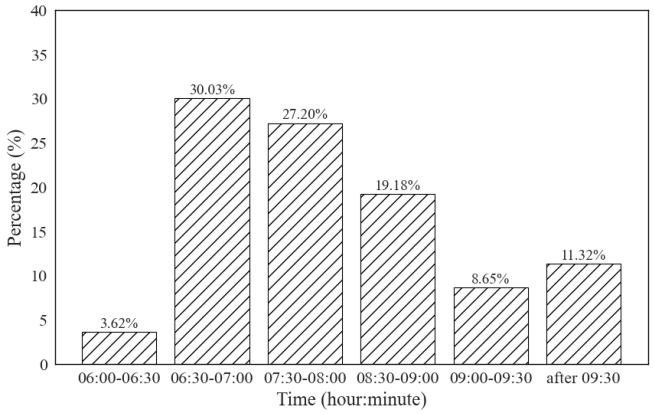


Fig. 4. Distribution of participants' wake-up time in the morning

TABLE II: Physiological parameters as features for NRSD analysis

| Feature name | Feature description | Relation with activities |
|---|---|---|
| SDRR | Standard deviation of RR interval | Measuring activities of SNS and PNS, mainly the activity of SNS [43] |
| RMSSD | RR Interval Difference Root Mean Square | Measuring activities of PNS [44] |
| Ave | Average of RRIS | Reflecting average level of ANS activity [45] |
| Var | Variance of RRIS | – |
| CVrr | Heart rate coefficient of variation | Reflecting the total tension of ANS activity [46] |
| SDAFD, MAFD, SDFD | Standard deviation of the absolute value of the first-order derivative of the RR interval [47]; Average of the absolute first-order differences of RRIS [47]; Standard deviation of the first-order difference of RRIS [47] | – |
| PNN50, PNN40, PNN30 PNN20, PNN10 | Percentage of the absolute differences between two adjacent normal RRI greater than 50, 40, 30, 20, 10 milliseconds | Measuring activities of PNS [43], [45], [48] |
| Fractality | The range between the maximum and minimum absolute local maxima in the wavelet coefficients of the RR interval sequence. | – |
| FD | Fractal dimension | Measuring the complexity of ANS activity [49] |
| PE, SampEnVal, Disten | Entropy of a permutation [50]; Sample entropy [51]; Conditional entropy [52] | Measuring activities of ANS |
| SD1, SD2, Cn, CCM | SD1, SD2, Cn and CCM indices of Poincare plots of RRIS | Short- and long- term HRV indicators to measure the volatility of ANS activity [53] |
| HR | Heart rate | Measuring the activity of PNS |
| RR_mod | Mean deviation of RR intervals relative to the mean value | Measuring the activity of PNS |
| HF1, HF2 | Mean value of power spectral density greater than the median between 0.2 Hz and 0.25 Hz [36]; Mean value of power spectral density greater than the median between 0.25 Hz and 0.35 Hz [36] | Measuring the activity of PNS |
| LF1 | Mean value of power spectral density greater than the median between 0.08 Hz and 0.12 Hz [36] | Mainly reflecting the activity of SNS |
| F1(n), F2(n) | Average fluctuation coefficients respectively in small scales n=1, 2, ..., 10; Average fluctuation coefficients respectively in large scales n=30, 31, ..., 50 | Measuring the fluctuations of RRIS at lag scales n, reflecting the complexity of ANS activity [48] |
| RLHE_3 | The third smallest of all negative peaks in the first-order difference of the local Hurst exponent of the RR interval sequence | Measuring the complexity of RRIS controlled by SNS and PNS competition [35] |
| LF, HF, AF | Power of the RRIS in 0.04-0.15 Hz calculated by Lomb-Scargle algorithm; Power of the RRIS in 0.15-0.4 Hz calculated by Lomb-Scargle algorithm; Power of the RRIS in 0.04-0.4 Hz | Mainly reflecting the activity of SNS [54], Measuring the activity of PNS [54], Measuring the total activity of ANS [54] |
| LF/HF, LF/AF, HF/AF | Ratio of LF and HF; Normalized LF; Normalized HF | Reflecting balance between SNS and PNS [43], Proportion of SNS activity in total ANS activity [45], Proportion of PNS activity in total ANS activity [45] |
| Sport_SDNN, Sport_AVE Sport_theta, Mean_fxyz | Standard deviation, Mean, Variance of AT-ACC, and Mean of AT-ACC greater than the median | – |

RRIS: RR interval series; ANS: autonomic nervous system; SNS: sympathetic nervous system; PNS: parasympathetic nervous system; PSD: power spectral density.

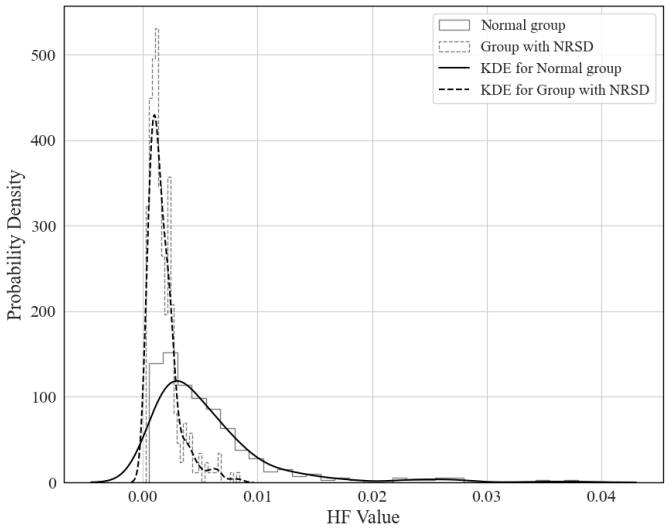


Fig. 5. Probability density and KDE of the 'HF' feature in a single time slot

CNN, which includes a two-dimensional convolutional layer with 8 filters of size 2×2, designed to capture multi-level and spatially diverse features. The subsequent ECA layer enhances the model's ability to prioritize critical features, thereby supporting improved classification performance.

Following these stages, the data enters the FCNN component. The 40×78 matrix is first flattened into a one-dimensional vector. To reduce overfitting, a Dropout layer with a rate of 0.2 is applied immediately after the input layer. The model then progresses through three Dense layers, each utilizing Scaled Exponential Linear Unit activation functions. The first hidden layer contains 80 neurons, followed by Batch Normalization to enhance training stability and speed. The second hidden layer has 64 neurons, while the third contains 30 neurons, with an additional Batch Normalization layer applied after these Dense layers. The architecture concludes with a Dense output layer containing two neurons, equipped with a softmax activation function to classify data into the 'with NRSD' and 'without NRSD' categories. The model structure is shown in Figure 6.

To ensure robust model generalization, we randomly partitioned the dataset into training, validation, and test sets with a 6:2:2 ratio. We ensured that data from the same participant was confined to a single dataset to prevent data leakage and overfitting. Model parameters were optimized based on the accuracy on the training set, while the training process was terminated when the accuracy on the validation set reached the maximum. Then, the trained model corresponding to the highest validation accuracy was tested on the test set to assess its generalization capability.

## III. Result

This section provides detailed results of the statistical analyses and machine learning techniques employed to identify NRSD conditions and quantify symptom severity.

### A. Effects of NRSD on Physiological Features

In addition to the 'HF' feature in Figure 7, Figures 8 and 9 present box plots for the 'MAFD' and 'pNN50' features, which highlight significant inter-group differences between the NRSD group and the normal group. The colored box plots indicate that, during phases of moderate to high PNS activation, the NRSD group demonstrates significantly lower PNS activation compared to the normal group. However, in phases of low PNS activation, the differences between the two groups become less pronounced.

### B. Binary Classification of Samples Labeled as 'with NRSD' and 'without NRSD'

Table III presents the performance metrics of the CNN_ECAnet model for binary classification of samples labeled as 'with NRSD' and 'without NRSD'. To assess the impact of each model component, we conducted an ablation study, demonstrating that the inclusion of CNN and ECA layers significantly enhances the performance of CNN_ECAnet compared to the standalone FCNN. Additionally, we performed the same binary classification using a classical Linear Discriminant Classifier (LDC). Table III also summarizes the performance metrics for the component-ablated models and the LDC model. The results show that the FCNN outperforms the LDC, indicating that a neural network model is better suited for NRSD detection. Furthermore, the models with component ablation exhibit decreased performance relative to CNN_ECAnet, underscoring the importance of integrating CNN and ECA components within the FCNN architecture. Table III shows that the false positive rate (FPR) of CNN_ECAnet is substantially higher than its false negative rate (FNR), indicating that while the model effectively detects true NRSD, its accuracy is impacted by false detection of NRSD. Since the 'without NRSD' category includes diverse subgroups—specifically, normal samples, samples with depression but no NRS, and samples with NRS but no depression—we further calculated the FPRs for each of these subgroups. The FPRs were 19.31%, 33.33%, and 75% for the 'normal', 'with depression but no NRS', and 'with NRS but no depression' groups, respectively. That is, the Fl score for differentiating 'with NRSD' from 'normal' is 83.02%.

### C. Severity Quantification of NRSD Using Posterior Probability

As illustrated in Figure 10, we calculated the mean and standard deviation of the posterior probability of NRSD for each time slot, comparing subjects with NRSD to those labeled as normal. The results indicate that subjects with NRSD exhibited significantly elevated posterior probabilities of NRSD, all exceeding 0.5, during periods likely associated with deep sleep, when PNS activation is moderate to high. In contrast, subjects without NRSD displayed notably lower posterior probabilities of NRSD, generally below 0.5, during phases of moderate to high PNS activation, suggesting restorative sleep. At lower levels of PNS activation, the posterior probabilities of NRSD for both groups tended to converge. Given that awake

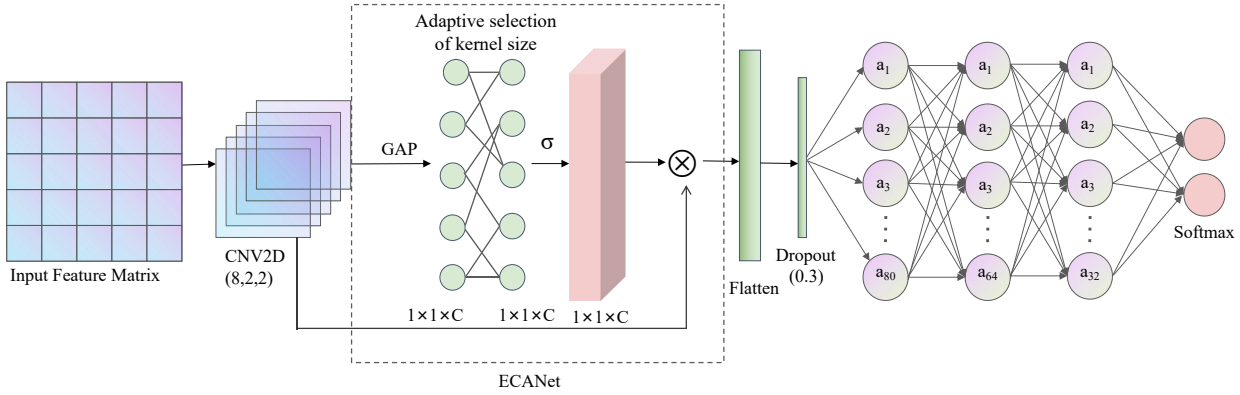


Fig. 6. CNN_ECAnet model structure

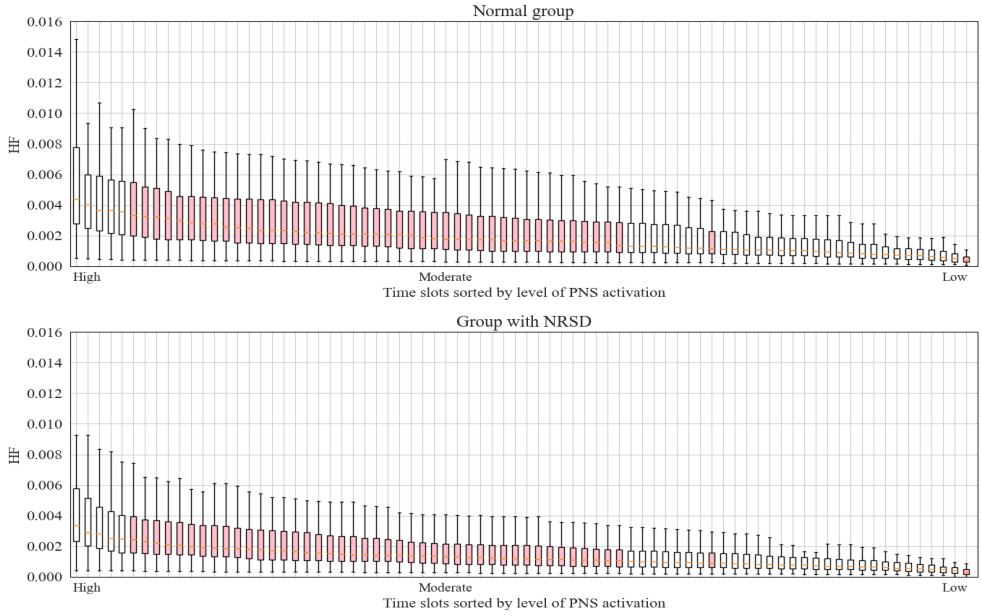


Fig. 7. Box plots of the 'HF' feature in the 78 nocturnal time slots

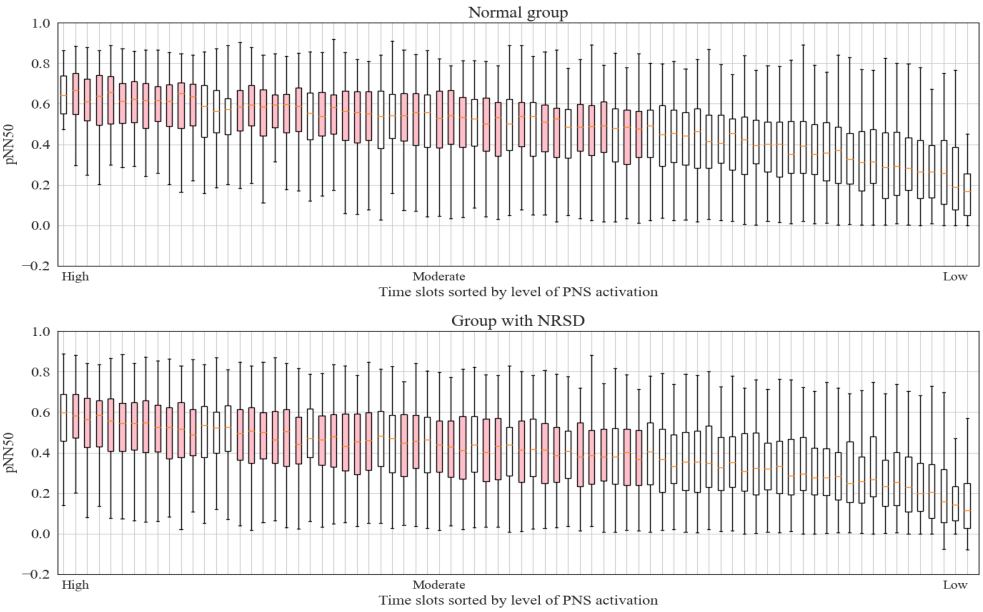


Fig. 8. Box plots of the 'PNN50' feature in the 78 nocturnal time slots

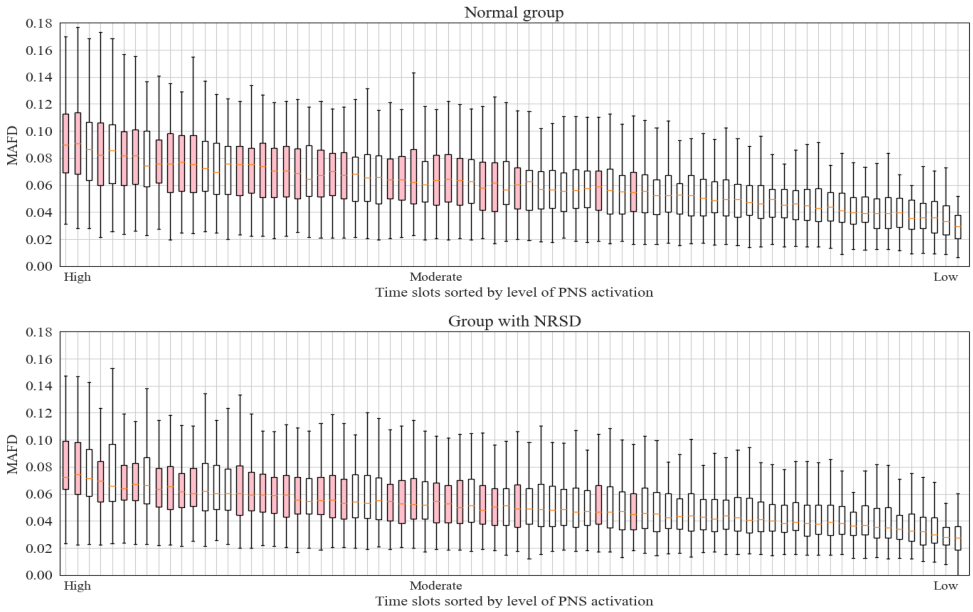


Fig. 9. Box plots of the 'MAFD' feature in the 78 nocturnal time slots

TABLE III: Performance Metrics of Different Models

| Model name | FPR | FNR | Acc | Prec | Spec | Sens | F1 |
|---|---|---|---|---|---|---|---|
| LDC | 40.35% | 41.94% | 59.09% | 43.90% | 59.65% | 58.06% | 50.00% |
| FCNN | 33.33% | 12.90% | 73.86% | 58.69% | 66.66% | 87.09% | 70.12% |
| CNN | 28.80% | 14.06% | 76.19% | 60.43% | 71.20% | 85.94% | 70.96% |
| CNN_ECAnet | 25.43% | 6.40% | 81.25% | 66.66% | 74.56% | 93.54% | 77.85% |

Samples from individuals with NRSD were the positive ones, and those from individuals without NRSD were the negative ones. FPR: false positive rate; FNR: false negative rate; Acc: ratio of correctly detected positive and negative samples to total samples; Prec: ratio of correctly detected positive samples to totally detected positive samples; Spec: ratio of correctly detected negative samples to total negative samples; Sens: ratio of correctly detected positive samples to total positive samples; F1: $2(\text{Prec} \times \text{Sens})/(\text{Prec} + \text{Sens})$.

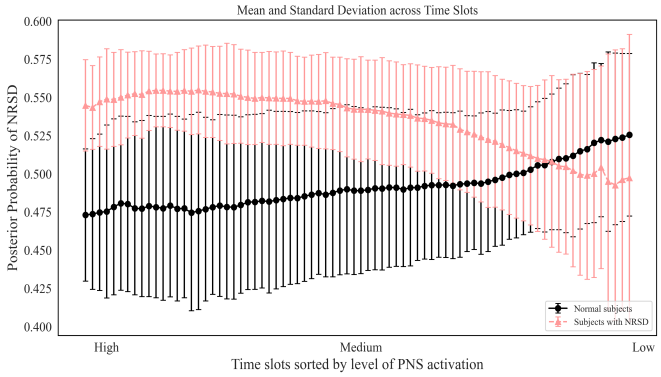


Fig. 10. Posterior Probabilities of NRSD calculated for two groups in 78 nocturnal time slots

and light sleep states correspond to lower PNS activation compared to deep sleep [56], [57], these findings suggest that the restorative effect of sleep is primarily determined by the level of PNS activation during deep sleep.

### D. A System for Automatic Analysis of NRSD

We developed an automated system for identifying NRSD and quantifying symptom severity, as illustrated in Figure 11. This system provides an efficient and non-invasive approach to sleep monitoring, covering signal acquisition, data preprocessing, feature extraction, and NRSD analysis. Signal acquisition is carried out using Shimmer devices, which capture HRV through ECG signals, or wearable watches that collect HRV data via photoplethysmography. The physiological data is then uploaded to a computer for NRSD analysis using the methodologies outlined in our research. The system enables users to access historical data by entering a username. Selected data are analyzed using the trained CNN_ECANet model and the posterior probability method described in our work, offering a detailed measure of NRSD for the chosen night, as depicted in Figure 11.

## IV. Discussion

Although NRSD is common among individuals with depressive symptoms, practical methods for daily NRSD screening using wearable sensing technology have been limited. This study presents a novel model, CNN_ECAnet, which leverages ECG and T-ACC signals to identify individuals with NRSD. Compared to prior models that detect MDD in daily life with a best-case FPR of 45% and an FNR of approximately 40% using deep learning on actigraphy data [58] and an F1 score of 81.9% using sleep photoplethysmography data [59],

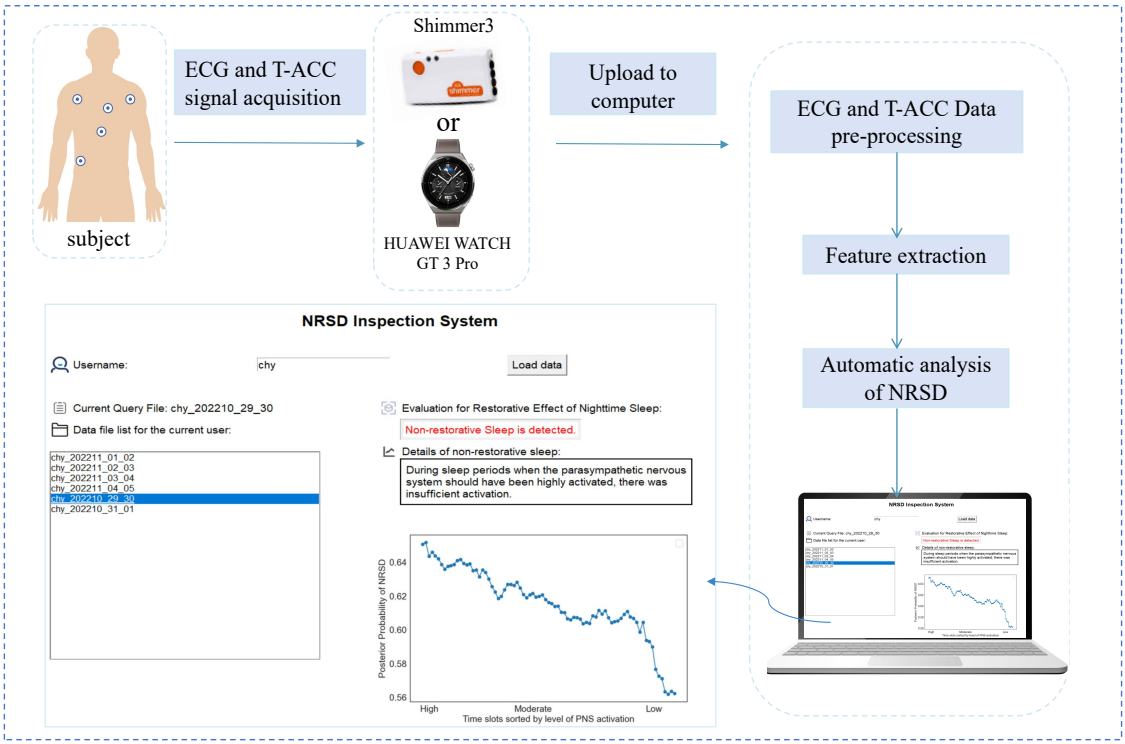


Fig. 11. Concept architecture of a system for automatic identification of NRSD

CNN_ECAnet demonstrates superior performance in detecting the specific symptom of NRS associated with depression. This model effectively distinguishes subject-independent samples due to two primary features.

First, to enhance data comparability across different sampling dates and individuals, we aligned data based on PNS activation levels. This approach eliminates the need for medical professionals to perform sleep staging, as was necessary in previous studies. Second, CNN_ECAnet incorporates an attention mechanism that selectively highlights critical features, allowing for precise quantification of neurophysiological activity related to NRSD. This model not only detects the presence of NRSD but also quantifies inadequate PNS activation using Bayesian posterior probabilities, providing an objective measure of NRSD severity through detailed visualization of PNS activation levels across nocturnal time slots.

Statistical tests conducted in this study revealed that, during expected moderate-to-high PNS activation periods, individuals with NRSD showed reduced HRV and lower PNS activation compared to those without NRSD. Given the established relationship between PNS activation and sleep quality and restorative capacity [60]–[62], these findings suggest that depression may impair the self-repair function of sleep, consistent with prior research [63]–[66]. This impairment could exacerbate psychological and physiological issues during waking hours in individuals with NRSD, emphasizing the importance of enhancing restorative sleep to alleviate depressive symptoms and improve overall health.

In this study, a small proportion (9 out of 149) of participants exhibited NRS on at least four nights per week without concurrent depression. These cases present challenges to CNN_ECAnet's accuracy, resulting in a higher FPR (75%) for this group. However, as NRS is a known risk factor for various mental and physical health conditions, including depression, such false positives may still be valuable for early screening and intervention.

Considering the relatively high FPRs for individuals with depression but no NRS and those with NRS but no depression, a practical application sequence for NRSD monitoring could be as follows: First, if CNN_ECAnet detects NRSD persisting for over two weeks, individuals would be advised to seek an expert consultation. During this consultation, individuals would report symptoms related to NRS, while experts could objectively evaluate these symptoms by reviewing posterior probabilities of NRSD over the preceding two weeks. Finally, during treatment, the change in posterior probabilities of NRSD would be monitored to assess the alleviation of NRS.

This study has the following limitations. The physiological dataset's sample size was insufficient for more complex deep learning techniques, which require extensive training data. Additionally, data collection was restricted to university students and postgraduates aged 18-25, limited the age and occupation diversity of the subjects. Furthermore, the data acquisition device used had a sampling rate of 512 Hz, whereas commercial wearable PPG devices typically have a sampling rate of 100 Hz. Thus, further validation with data from wearable PPG devices is necessary before practical implementation.

## V. Conclusion

This work proposed a machine learning model for effectively identifying NRSD using ECG and T-ACC signals. This model captured critical neurophysiological and physical

activity features, offering quantitative insights into restorative effects of sleep via a graphical user interface. By leveraging physiological data that are more readily available in daily life, our model provides a novel and practical tool for NRSD evaluation.

## VI. ACKNOWLEDGMENT

The authors would like to thank the subjects involved in the data collection for this work, as well as the graduate students involved in operating the data collection and pre-processing; this work was funded by the National Natural Science Foundation of China (Grant No. 62176219, 61872301).

## REFERENCES

[1] D. Vigo, G. Thornicroft, and R. Atun, "Estimating the true global burden of mental illness," *Lancet Psychiatry*, vol. 3, no. 2, pp. 171–178, 2016.

[2] C. G. Davey and P. D. McGorry, "Early intervention for depression in young people: a blind spot in mental health care," *Lancet Psychiatry*, vol. 6, no. 3, pp. 267–272, 2019.

[3] P. Cuijpers, A. Stringaris, and M. Wolpert, "Treatment outcomes for depression: challenges and opportunities," *Lancet Psychiatry*, vol. 7, no. 11, pp. 925–927, 2020.

[4] B. A. Gaudiano, D. Young, I. Chelminski, and M. Zimmerman, "Depressive symptom profiles and severity patterns in outpatients with psychotic vs nonpsychotic major depression," *Compr. Psychiat.*, vol. 49, no. 5, pp. 421–429, 2008.

[5] G. Parker, G. Malhi, D. Hadzi-Pavlovic, and K. Parker, "Sleeping in? the impact of age and depressive sub-type on hypersomnia," *J. Affect. Disord.*, vol. 90, no. 1, pp. 73–76, 2006.

[6] J. Angst, A. Gamma, F. Benazzi, V. Ajdacic, and W. Rössler, "Melancholia and atypical depression in the zurich study: epidemiology, clinical characteristics, course, comorbidity and personality," *Acta Psychiatr. Scand.*, vol. 115, pp. 72–84, 2007.

[7] A. Murru, G. Guiso, M. Barbuti, G. Anmella, N. Verdolini, L. Samalin, J.-M. Azorin, J. J. Angst, C. L. Bowden, S. Mosolov, *et al.*, "The implications of hypersomnia in the context of major depression: results from a large, international, observational study," *Eur. Neuropsychopharmacol.*, vol. 29, no. 4, pp. 471–481, 2019.

[8] J. S. Carpenter, J. J. Crouse, E. M. Scott, S. L. Naismith, C. Wilson, J. Scott, K. R. Merikangas, and I. B. Hickie, "Circadian depression: a mood disorder phenotype," *Neurosci. Biobehav. Rev.*, vol. 126, pp. 79–101, 2021.

[9] P. C. Zee, H. Attarian, and A. Videnovic, "Circadian rhythm abnormalities," *Continuum (Minneap. Minn.)*, vol. 19, no. 1, pp. 132–147, 2013.

[10] G. D. Potter, D. J. Skene, J. Arendt, J. E. Cade, P. J. Grant, and L. J. Hardie, "Circadian rhythm and sleep disruption: causes, metabolic consequences, and countermeasures," *Endocr. Rev.*, vol. 37, no. 6, pp. 584–608, 2016.

[11] B. L. Mason, A. Davidov, A. Minhajuddin, and M. H. Trivedi, "Focusing on insomnia symptoms to better understand depression: A star* d report," *J. Affect. Disord.*, vol. 260, pp. 183–186, 2020.

[12] N. F. Zaki, D. W. Spence, A. S. BaHammam, S. R. Pandi-Perumal, D. P. Cardinali, and G. M. Brown, "Chronobiological theories of mood disorder," *Eur. Arch. Psych. Clin. Neurosci.*, vol. 268, pp. 107–118, 2018.

[13] T. Roth, S. Jaeger, R. Jin, A. Kalsekar, P. E. Stang, and R. C. Kessler, "Sleep problems, comorbid mental disorders, and role functioning in the national comorbidity survey replication," *Biol. Psychiatry*, vol. 60, no. 12, pp. 1364–1371, 2006.

[14] M. M. Ohayon and S.-C. Hong, "Prevalence of insomnia and associated factors in south korea," *J. Psychosomat. Res.*, vol. 53, no. 1, pp. 593–600, 2002.

[15] P. Meerlo, R. Havekes, and A. Steiger, "Chronically restricted or disrupted sleep as a causal factor in the development of depression," *Sleep, neuronal plasticity and brain function*, pp. 459–481, 2015.

[16] R. C. Cox and B. O. Olatunji, "A systematic review of sleep disturbance in anxiety and related disorders," *J. Anxiety Disord.*, vol. 37, pp. 104–129, 2016.

[17] T. Kawada, "Feeling refreshed by sleep can predict psychological well-being assessed using the general health questionnaire in male workers: A 3-year follow-up study," *Psychiatry Investig.*, vol. 9, no. 4, p. 418, 2012.

[18] J. H. Park, J.-H. Yoo, and S. H. Kim, "Associations between non-restorative sleep, short sleep duration and suicidality: Findings from a representative sample of k orean adolescents," *Psychiatry Clin. Neurosci.*, vol. 67, no. 1, pp. 28–34, 2013.

[19] E. M. Boland, J. R. Vittengl, L. A. Clark, M. E. Thase, and R. B. Jarrett, "Is sleep disturbance linked to short-and long-term outcomes following treatments for recurrent depression?," *J. Affect. Disord.*, vol. 262, pp. 323–332, 2020.

[20] P. Monteleone, V. Martiadis, and M. Maj, "Circadian rhythms and treatment implications in depression," *Prog. Neuro-Psychopharmacol. Biol. Psychiatry*, vol. 35, no. 7, pp. 1569–1574, 2011.

[21] A. Steiger and M. Kimura, "Wake and sleep EEG provide biomarkers in depression," *J. Psychiatr. Res.*, vol. 44, no. 4, pp. 242–252, 2010.

[22] F. S. de Aguiar Neto and J. L. G. Rosa, "Depression biomarkers using non-invasive EEG: A review," *Neurosci. Biobehav. Rev.*, vol. 105, pp. 83–93, 2019.

[23] Y. Zhang, K. Wang, Y. Wei, X. Guo, J. Wen, and Y. Luo, "Minimal EEG channel selection for depression detection with connectivity features during sleep," *Comput. Biol. Med.*, vol. 147, p. 105690, 2022.

[24] M. Saad, L. B. Ray, B. Bujaki, A. Parvaresh, I. Palamarchuk, J. De Koninck, A. Douglass, E. K. Lee, L. J. Soucy, S. Fogel, *et al.*, "Using heart rate profiles during sleep as a biomarker of depression," *BMC psychiatry*, vol. 19, pp. 1–11, 2019.

[25] M. Saad, L. B. Ray, M. Bradley-Garcia, I. S. Palamarchuk, A. Gholamrezaei, A. Douglass, E. K. Lee, L. Soucy, and R. Robillard, "Autonomic modulation of cardiac activity across levels of sleep depth in individuals with depression and sleep complaints," *Psychosom. Med.*, vol. 82, no. 2, pp. 172–180, 2020.

[26] J. Shen, X. Zhang, G. Wang, Z. Ding, and B. Hu, "An improved empirical mode decomposition of electroencephalogram signals for depression detection," *IEEE Trans. Affect. Comput.*, vol. 13, no. 1, pp. 262–271, 2019.

[27] R. W. Logan and C. A. McClung, "Rhythms of life: circadian disruption and brain disorders across the lifespan," *Nat. Rev. Neurosci.*, vol. 20, no. 1, pp. 49–65, 2019.

[28] S. Fattinger, T. T. de Beukelaar, K. L. Ruddy, C. Volk, N. C. Heyse, J. A. Herbst, R. H. Hahnloser, N. Wenderoth, and R. Huber, "Deep sleep maintains learning efficiency of the human brain," *Nat. Commun.*, vol. 8, no. 1, p. 15405, 2017.

[29] S. Grubb and M. Lauritzen, "Deep sleep drives brain fluid oscillations," *Sci.*, vol. 366, no. 6465, pp. 572–573, 2019.

[30] T. A. Mellman, K. A. Bell, S. H. Abu-Bader, and I. Kobayashi, "Neighborhood stress and autonomic nervous system activity during sleep," *Sleep*, vol. 41, no. 6, p. zsy059, 2018.

[31] W. W. Zung, "A self-rating depression scale," *Arch. Gen. Psychiatry*, vol. 12, no. 1, pp. 63–70, 1965.

[32] X. Liu, "The application of the self-rating depression scale in the diagnosis of depression," *Chinese Journal of Aerospace Medicine*, vol. 3, no. 6, pp. 39–40, 2001. in Chinese.

[33] C. Wang, Z. Cai, and Q. Xu, "Analysis of 1340 normal individuals using the self-rating depression scale," *Chinese Journal of Neuropsychiatric Disorders*, vol. 12, no. 5, pp. 267–268, 1986. in Chinese.

[34] W. Wen, B. Li, and G. Liu, "Method, device, electronic equipment, and computer-readable storage medium for detecting sleepiness," October 2023. Chinese Invention Patent, number 202310905866.6.

[35] W. Wen, G. Liu, Z.-H. Mao, W. Huang, X. Zhang, H. Hu, J. Yang, and W. Jia, "Toward constructing a real-time social anxiety evaluation system: Exploring effective heart rate features," *IEEE Trans. Affect. Comput.*, vol. 11, no. 1, pp. 100–110, 2018.

[36] J. Li, M. Wang, F. Zhang, G. Liu, and W. Wen, "Chronic stress recognition based on time-slot analysis of ambulatory electrocardiogram and tri-axial acceleration," *IEEE Transactions on Affective Computing*, 2023.

[37] P. De Looff, L. Cornet, P. Embregts, H. Nijman, and H. Didden, "Associations of sympathetic and parasympathetic activity in job stress and burnout: A systematic review," *PLoS One*, vol. 13, no. 10, p. e0205741, 2018.

[38] G. Zoccoli and R. Amici, "Sleep and autonomic nervous system," *Curr. Opin. Physiol.*, vol. 15, pp. 128–133, 2020.

[39] H.-J. Tsai, T. B. Kuo, G.-S. Lee, and C. C. Yang, "Efficacy of paced breathing for insomnia: enhances vagal activity and improves sleep quality," *Psychophysiology*, vol. 52, no. 3, pp. 388–396, 2015.

[40] J. Trinder, J. Kleiman, M. Carrington, S. Smith, S. Breen, N. Tan, and Y. Kim, "Autonomic activity during human sleep as a function of time and sleep stage," *J. Sleep Res.*, vol. 10, no. 4, pp. 253–264, 2001.

[41] A. Baharav, S. Kotagal, V. Gibbons, B. Rubin, G. Pratt, J. Karin, and S. Akselrod, "Fluctuations in autonomic nervous activity during sleep displayed by power spectrum analysis of heart rate variability," *Neurology*, vol. 45, no. 6, pp. 1183–1187, 1995.

[42] Z. Shinar, S. Akselrod, Y. Dagan, and A. Baharav, "Autonomic changes during wake–sleep transition: A heart rate variability based approach," *Auton. Neurosci.*, vol. 130, no. 1-2, pp. 17–27, 2006.

[43] A. L. Goldberger, L. A. Amaral, L. Glass, J. M. Hausdorff, P. C. Ivanov, R. G. Mark, J. E. Mietus, G. B. Moody, C.-K. Peng, and H. E. Stanley, "Physiobank, physiotoolkit, and physionet: components of a new research resource for complex physiologic signals," *circulation*, vol. 101, no. 23, pp. e215–e220, 2000.

[44] M. Hillmert, A. Bergmüller, A. Minow, J. Raggatz, and I. Böckelmann, "Psychophysiologische beanspruchungskorrelate während kognitiver belastung," *Zbl Arbeitsmed*, vol. 70, pp. 149–163, 2020.

[45] M. N. Jarczok, K. Weimer, C. Braun, D. P. Williams, J. F. Thayer, H. O. Gündel, and E. M. Balint, "Heart rate variability in the prediction of mortality: A systematic review and meta-analysis of healthy and patient populations," *Neurosci. Biobehav. Rev.*, vol. 143, p. 104907, 2022.

[46] D. Razanskaite-Virbickiene, E. Danyte, G. Mockeviciene, R. Dobrovolskiene, R. Verkauskiene, and R. Zalinkevicius, "Can coefficient of variation of time-domain analysis be valuable for detecting cardiovascular autonomic neuropathy in young patients with type 1 diabetes: A case control study," *BMC Cardiovasc. Disord.*, vol. 17, pp. 1–9, 2017.

[47] J. Zhu, L. Ji, and C. Liu, "Heart rate variability monitoring for emotion and disorders of emotion," *Physiol. Meas.*, vol. 40, no. 6, p. 064004, 2019.

[48] J. Xie, W. Wen, G. Liu, and Y. Li, "Intelligent biological alarm clock for monitoring autonomic nervous recovery during nap," *Int. J. Comput. Intell. Syst.*, vol. 12, no. 2, pp. 453–459, 2019.

[49] Z. Hua, C. Chen, R. Zhang, G. Liu, and W. Wen, "Diagnosing various severity levels of congestive heart failure based on long-term hrv signal," *Appl. Sci.*, vol. 9, no. 12, p. 2544, 2019.

[50] F. Chen, L. Zhao, B. Li, and L. Yang, "Depression evaluation based on prefrontal EEG signals in resting state using fuzzy measure entropy," *Physiol. Meas.*, vol. 41, no. 9, p. 095007, 2020.

[51] J. S. Richman and J. R. Moorman, "Physiological time-series analysis using approximate entropy and sample entropy," *Am. J. Physiol. Heart Circ. Physiol.*, vol. 278, no. 6, pp. H2039–H2049, 2000.

[52] C. Yan, P. Li, M. Yang, Y. Li, J. Li, H. Zhang, and C. Liu, "Entropy analysis of heart rate variability in different sleep stages," *Entropy*, vol. 24, no. 3, p. 379, 2022.

[53] C. K. Karmakar, A. H. Khandoker, J. Gubbi, and M. Palaniswami, "Complex correlation measure: A novel descriptor for poincaré plot," *Biomed. Eng. Online*, vol. 8, pp. 1–12, 2009.

[54] Z. Hua, C. Chen, R. Zhang, G. Liu, and W. Wen, "Diagnosing various severity levels of congestive heart failure based on long-term HRV signal," *Appl. Sci.*, vol. 9, no. 12, p. 2544, 2019.

[55] T. Hastie, R. Tibshirani, and J. H. Friedman, "Kernel density estimation and classification," in *The Elements of Statistical Learning: Data Mining, Inference, and Prediction*, ch. 6, pp. 182–186, New York, NY, USA: Springer, 2 ed., 2009.

[56] M. Bonnet and D. Arand, "Heart rate variability: sleep stage, time of night, and arousal influences," *Electroencephalography and clinical neurophysiology*, vol. 102, no. 5, pp. 390–396, 1997.

[57] F. Iellamo, F. Placidi, M. G. Marciani, A. Romigi, M. Tombini, S. Aquilani, M. Massaro, A. Galante, and J. M. Legramante, "Baroreflex buffering of sympathetic activation during sleep: evidence from autonomic assessment of sleep macroarchitecture and microarchitecture," *Hypertension*, vol. 43, no. 4, pp. 814–819, 2004.

[58] G. D. Price, M. V. Heinz, A. C. Collins, and N. C. Jacobson, "Detecting major depressive disorder presence using passively-collected wearable movement data in a nationally-representative sample," *Psychiatry research*, vol. 332, p. 115693, 2024.

[59] S. Sato, T. Hiratsuka, K. Hasegawa, K. Watanabe, Y. Obara, N. Kariya, T. Shinba, and T. Matsui, "Screening for major depressive disorder using a wearable ultra-short-term HRV monitor and signal quality indices," *Sensors*, vol. 23, no. 8, p. 3867, 2023.

[60] H. U. Dissanayake, Y. S. Bin, S. Ucak, P. de Chazal, K. Sutherland, and P. A. Cistulli, "Association between autonomic function and obstructive sleep apnea: a systematic review," *Sleep Med. Rev.*, vol. 57, p. 101470, 2021.

[61] M. de Zambotti, J. Trinder, A. Silvani, I. M. Colrain, and F. C. Baker, "Dynamic coupling between the central and autonomic nervous systems during sleep: a review," *Neurosci. Biobehav. Rev.*, vol. 90, pp. 84–103, 2018.

[62] S. J. Fatt, J. E. Beilharz, M. Joubert, C. Wilson, A. R. Lloyd, U. Vollmer-Conna, and E. Cvejic, "Parasympathetic activity is reduced during slow-wave sleep, but not resting wakefulness, in patients with chronic fatigue syndrome," *J. Clin. Sleep Med.*, vol. 16, no. 1, pp. 19–28, 2020.

[63] W. Cheng, E. T. Rolls, H. Ruan, and J. Feng, "Functional connectivities in the brain that mediate the association between depressive problems and sleep quality," *JAMA psychiatry*, vol. 75, no. 10, pp. 1052–1061, 2018.

[64] S. R. Pandi-Perumal, J. M. Monti, D. Burman, R. Karthikeyan, A. S. BaHammam, D. W. Spence, G. M. Brown, and M. Narashimhan, "Clarifying the role of sleep in depression: A narrative review," *Psychiatr. Res.*, vol. 291, p. 113239, 2020.

[65] M. Saad, L. B. Ray, M. Bradley-Garcia, I. S. Palamarchuk, A. Gholamrezaei, A. Douglass, E. K. Lee, L. Soucy, and R. Robillard, "Autonomic modulation of cardiac activity across levels of sleep depth in individuals with depression and sleep complaints," *PSYCHOSOM MED*, vol. 82, no. 2, pp. 172–180, 2020.

[66] I. B. Hickie and N. L. Rogers, "Novel melatonin-based therapies: potential advances in the treatment of major depression," *Lancet*, vol. 378, no. 9791, pp. 621–631, 2011.